

## TEXTURE EVOLUTION DURING PROCESSING OF A 3004 ALUMINIUM ALLOY

Cl. MAURICE <sup>+</sup>, J.H. DRIVER <sup>+</sup>, G.M. RAYNAUD \*  
and Ph. LEQUEU \*

<sup>+</sup> Materials Department, Ecole des Mines de Saint-Etienne  
158 cours Fauriel, 42023 Saint-Etienne, France.

\* Centre de Recherches de Voreppe S.A., Pechiney,  
BP 27, 38340 Voreppe, France.

### ABSTRACT

Macroscopic texture changes were measured on cold rolled and recrystallized samples of a 3004 alloy using X-ray pole figures converted into ODFs by means of the standard spherical harmonics method. Local textures were also estimated using electron diffraction techniques : TEM, SACP and EBSP. The initial recrystallized starting material with a relatively strong cube texture was rolled to strains of 0.6 and 3, reducing the cube component and increasing the  $\beta$ -fibre rolling texture components. On annealing the subsequent recrystallization texture behaviour depends upon the prior strain and the heating rate. After relatively low strains, particle stimulated nucleation occurred giving rise to an almost random texture. After high rolling strains nucleation appears to occur on both particles and in transition bands ; the latter favour the creation of new cube grains. Finally, low heating rates which allow extensive recovery before recrystallization have been shown to decrease significantly the cube texture component.

### 1. INTRODUCTION

The recrystallization of 3004 aluminium alloys can be used to control the earing behaviour of these alloys but a successful treatment requires a knowledge of the mechanisms that govern the texture evolution from the deformed to the recrystallized, or partially recrystallized state. The aim of the present study is to quantitatively identify the significant microstructural and texture parameters - at both the macroscopic and microscopic scales - during recrystallization of this type of alloy and hence identify the controlling mechanisms.

Particular attention will be paid to the sites and orientations of the recrystallized nuclei as a function of rolling strain, heating conditions and metallurgical parameters such as the particle distribution and the initial textures, both macroscopic and local.

## 2. ALLOY AND PROCESSING CONDITIONS

A standard commercial 3004 alloy was used of composition : Mn 1.04%, Mg 1.09%, Fe 0.42%, Si 0.18% (wt%). The alloy was provided in the form of 2.7 mm recrystallized sheet, obtained after DC casting, by homogenising and hot rolling to 2.7 mm.

The initial microstructure is characterised by a bimodal precipitate (Al-Fe-Mn-Si type) distribution made up of coarse (5 to 15  $\mu\text{m}$ ) particles formed during solidification and fine (0.2 to 1  $\mu\text{m}$ ) particles precipitated during homogenisation. The grain size was heterogeneous (10 to 50  $\mu\text{m}$ ), and the initial texture exhibited a relatively strong cube component ( $\sim 32\%$  cube plus a weak 6% Bs-S residual rolling component and  $f_{\text{max}} \sim 11.5$ ).

This alloy was cold rolled to Von Mises equivalent strains  $\bar{\epsilon}$  of 0.6 and 3, and then recrystallized either isothermally in a salt bath or during an industrial type slow heating rate cycle ( $\sim 40^\circ\text{C/h}$ ).

## 3. RECRYSTALLIZATION KINETICS

Recrystallization kinetics after cold rolling to strains of 0.6 and 3 were evaluated by Vickers microhardness measurements on samples isothermally annealed in the temperature range 200 to 350  $^\circ\text{C}$ , Figure 1. Note the significant hardness decrease that occurs before the large drop due to recrystallization as a consequence of recovery processes at either lower temperatures ( $T < 275^\circ\text{C}$ ) or short times ( $T > 275^\circ\text{C}$ ). This high degree of recovery, particularly after  $\bar{\epsilon} = 3$  is consistent with the recent analysis of Furu, Marthinsen and Nes <sup>(1)</sup> and is corroborated by differential scanning calorimetry (DSC) measurements of the stored energies carried out by A.M. Zahra (CTM, Marseille). Stored energies are of the order of 35 J/mole after  $\bar{\epsilon} = 0.6$  and 50 J/mole after  $\bar{\epsilon} = 3$ . Furthermore, whereas after  $\bar{\epsilon} = 0.6$  the energies released during recovery and recrystallization are roughly equivalent, it is significant that after  $\bar{\epsilon} = 3$  recovery appears to release about 3 times as much energy as recrystallization. This recovery behaviour is expected to occur to a large extent during the slow heating rate cycle.

The annealing treatments selected for detailed microstructural and texture investigations are also indicated on Figure 1 :  $\bar{\epsilon} = 0.6$ ,  $T = 315^\circ\text{C}$  and  $\bar{\epsilon} = 3$ ,  $T = 290^\circ\text{C}$ ; in both cases recrystallization begins after about  $10^2$  s. and finishes after about  $10^3$  s.

## 4. MACROSCOPIC TEXTURES

Macroscopic texture components were determined from X-ray pole figures obtained using the Dosophatex 4 circles equipment mounted on a standard texture goniometre. The pole figures were converted to ODFs using the spherical harmonics method, see for example Lücke et al.<sup>(2)</sup>. The volume fractions of the texture components were also evaluated from the  $C_l^{mn}$  coefficients by means of Gauss model functions. To simplify the presentation, most of the texture results are given here in terms of  $f(g)$  along the  $\beta$ -fibre rolling texture components between Cu  $\{112\}\langle 111\rangle$  and Bs  $\{011\}\langle 211\rangle$  and also, to indicate the behaviour of the recrystallization components,

along the cube-RD rotation direction between cube and Goss  $\{011\}\langle 100\rangle$ . The highest  $f$  values usually occur along one or other of these two lines.

The texture changes during cold rolling are illustrated in Figure 2. The usual increase in the  $\beta$ -fibre components, particularly at high strains is shown in 2(a). The concomitant decrease of the cube component can be seen in 2(b). This behaviour is consistent with Taylor - type rolling textures predictions; a recent modification of the RC (Relaxed Constraints) model has in fact been very successful in quantitatively predicting the ODF evolution for this type of alloy from  $\bar{\epsilon} = 0$  through to  $\bar{\epsilon} = 3$  (Maurice, Driver and Toth (3)).

Figure 3 illustrates the texture evolution on subsequent annealing. These  $f(g)$  plots include the results of isothermal annealing after  $\bar{\epsilon} = 3$  ( for different times up to recrystallization) and also the slow heating rate cycle for both  $\bar{\epsilon} = 0.6$  and  $\bar{\epsilon} = 3$ . Figure 3(a) clearly demonstrates the decrease of all the  $\beta$ -fibre components, as expected. The  $\beta$ -fibre section shows little difference between the isothermal and anisothermal heating results. However the  $f(g)$  plot along the cube-RD rotation direction, figure 3(b) illustrates a significant difference in the recrystallization behaviour between flash annealing and slow heating. The relatively strong  $\{012\}\langle 100\rangle$  and  $\{011\}\langle 100\rangle$  components after deformation  $\bar{\epsilon} = 3$  are considerably reduced by isothermal annealing at 290 °C while the cube component is reinforced up to 11%. In contrast slow heating has little effect on the intermediate  $\{012\}\langle 100\rangle$  texture and only very small quantities (<5%) of the cube texture are developed.

## 5. MICROSCOPIC INVESTIGATIONS

Local microstructures and grain orientations were examined on selected samples after isothermal annealing by a combination of standard TEM and more recent SEM microdiffraction techniques. The SEM techniques were selected area channelling patterns SACP on annealed grain nuclei  $> 10 \mu\text{m}$  and electron back scattered patterns EBSD on material with grains or subgrains  $> 0.5 \mu\text{m}$ . SACP patterns were interpreted using the Channel software developed by Schmidt and Olesen (4).

After a strain of 0.6 both optical and electron metallography of partially recrystallized samples reveal clear evidence for particle stimulated nucleation of new grains at the relatively coarse elongated particles, figure 4a. A study of the orientations of these new grains by SACP shows in fact that the grains nucleated in the vicinity of the large particles have virtually random orientations, figure 4b , in agreement with the results of Humphreys and Juul Jensen (5) and others.

After a strain of 3 a somewhat different behaviour is observed. Optical metallography indicates grain nucleation at large constituent particles and along deformation bands -probably transition bands- in the matrix. EBSD was used to identify the nucleation site orientations in this case and the results are shown in figure 5. There is evidence of cube nuclei forming in the transition bands between symmetrically oriented Cu - S components . When taken with the macroscopic texture changes, ie the decrease of the  $\beta$ -fibre components and an increase in cube, these local orientation results tend to confirm the conclusions of Ridha and Hutchinson (6) and Dons and Nes (7) according to which cube grains originate from transition bands. The latter are created, in part, by the decomposition of near cube oriented grains during rolling as a consequence of initial rotations of opposite sign about TD ( Akef and Driver (8) ), and then at higher strains by rotations towards complementary near S orientations.

TEM on sheet plane sections of the above rolled and partially recrystallized samples provide strong evidence for the importance of recovery processes. As a function of annealing time the following recovery stages are observed successively : (i) screw dislocation annihilation, (ii) polygonisation around second phase particles, (iii) generalised polygonisation and (iv) recrystallization.

The preferential recovery by polygonisation close to the particles indicates a possible explanation of the effect of recovery on recrystallization texture development (cf section 2). Rapid polygonisation near the particles at lower temperatures, before the recrystallization temperature is attained, may favour nucleation at particles rather than in transition bands and hence the low cube texture content after the slow heating rate cycle.

## 6. CONCLUSIONS

The results of this on-going study of macroscopic and local texture changes during rolling and recrystallization of a 3004 alloy can be summarised as follows :

- the cold rolling texture evolution is quantitatively consistent with a RC Taylor - type model up to strains of 3.
- isothermal recrystallization after a relatively low rolling strain leads to particle stimulated nucleation and a near random recrystallization texture.
- after high rolling strains and isothermal annealing, a relatively strong cube component is developed probably as a consequence of nucleation within transition bands.
- during a slow heating rate cycle significant recovery precedes recrystallization ; this appears to markedly alter the resulting texture and leads to a much weaker cube component.

## 7. ACKNOWLEDGEMENTS

The authors wish to thank Mme A.M. Zahra (CTM Marseille, France) for the accurate DSC analyses and also Professor E. Nes and colleagues for time on the EBSP equipment at SINTEF, Trondheim, Norway. Ms Maurice gratefully acknowledges the support of CRV (Pechiney) in the form of a CIFRE graduate student grant.

## 8. REFERENCES

1. T. Furu, K. Marthinsen and E. Nes, *Acta metall.*, to be published.
2. K. Lücke, J. Pospiech, K.H. Virnich and J.Jura, *Acta metall.*, **29**, 167 (1981)
3. C. Maurice, J. Driver and L. Toth, to be published.
4. N.H. Schmidt and N.O. Olesen, *Canadian Mineralogist*, **27**, 15, (1989)
5. F.J. Humphreys and D. Juul Jensen, *Annealing Processes - Recovery, Recrystallization and Grain Growth*, Proc. 7<sup>th</sup> Riso Int. Symp. 1986, pp 93-106.
6. A.A. Ridha and W.B. Hutchinson, *Acta metall.*, **30**, 1929, (1982)
7. A.L. Dons and E. Nes, *Mater. Sci. Techn.*, **2**, 8, (1986)
8. A. Akef and J.Driver, *Mater Sci. Eng.*, in press
9. J. Starkey, *Can. J. Earth Sci.*, **14**, 268 (1977)

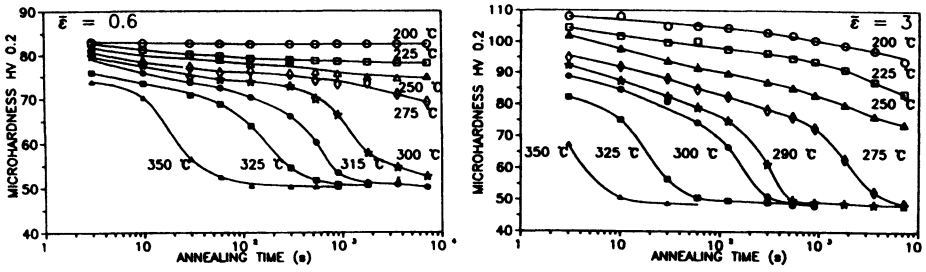


Fig 1 Hardness vs annealing time for flash annealing treatments in the temperature range 200 to 350 °C

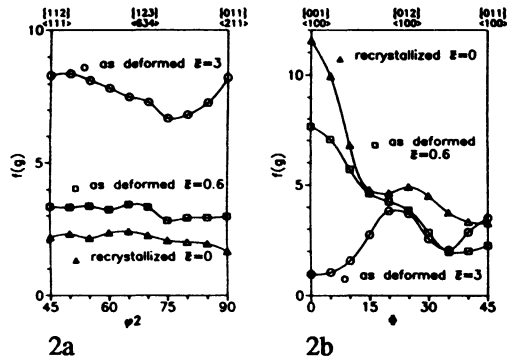


Fig 2 Texture Evolution during Cold Rolling - (a)  $\beta$ -fibre rolling texture components - (b) Cube RD Rotation ( $\phi_1 = 0^\circ$  and  $\phi_2 = 0^\circ$ )

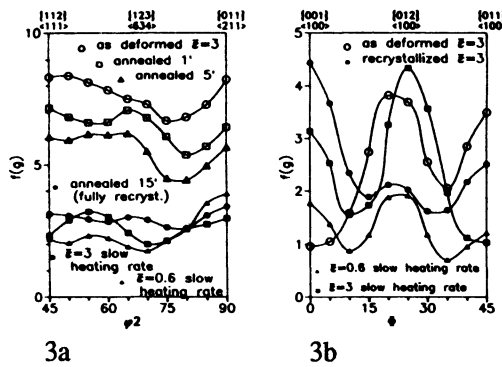


Fig 3 Texture Evolution during Annealing - (a)  $\beta$ -fibre - Isothermal anneal at 290 °C for  $\bar{\epsilon}=3$  (1', 5' and 15') + fully recrystallized samples after an industrial anneal for  $\bar{\epsilon} = 0.6$  and 3 - (b) Cube RD Rotation

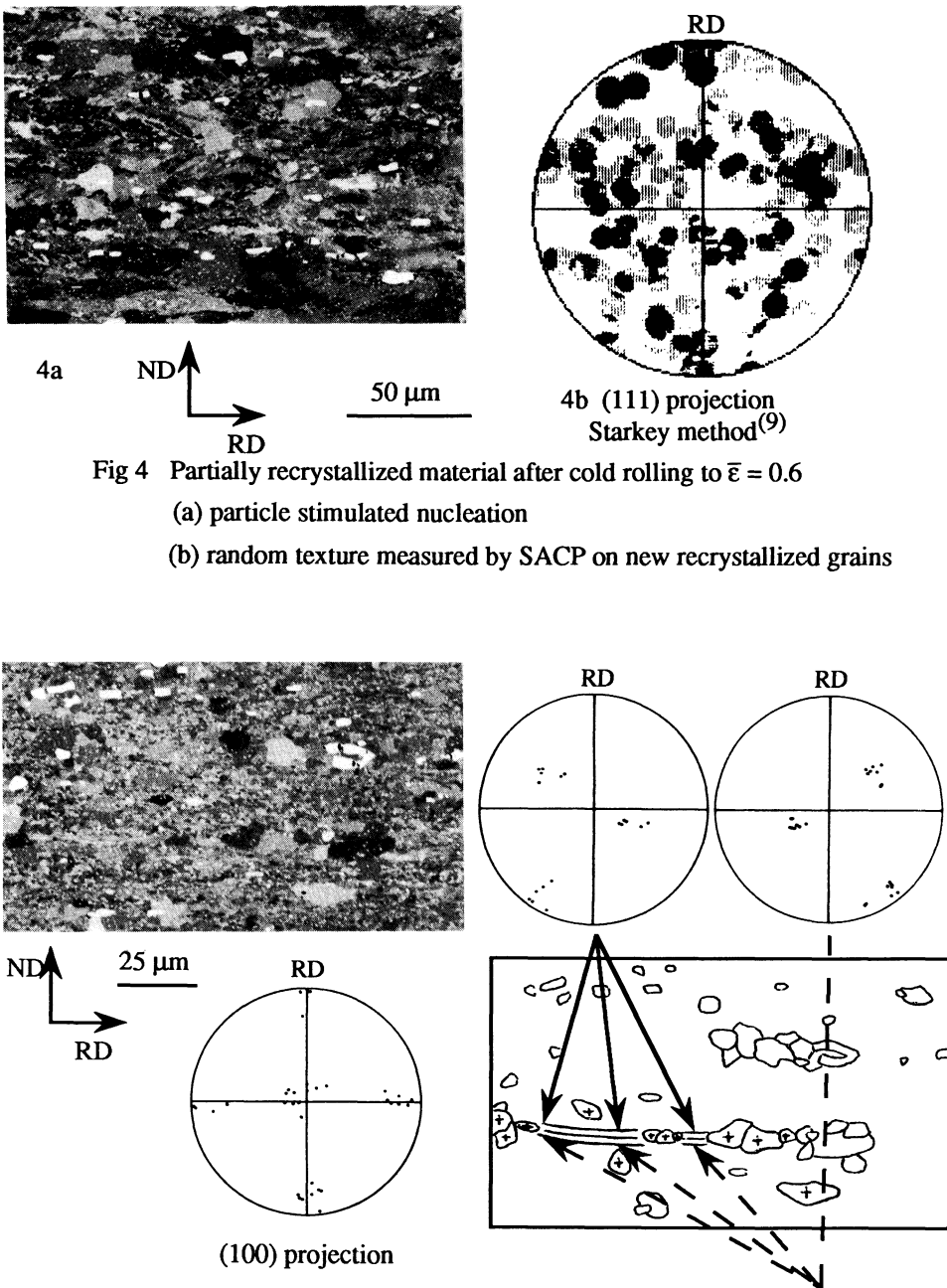


Fig 4 Partially recrystallized material after cold rolling to  $\bar{\epsilon} = 0.6$

(a) particle stimulated nucleation

(b) random texture measured by SACP on new recrystallized grains

Fig 5 Partially recrystallized material after cold rolling to  $\bar{\epsilon} = 3$ .

Cube oriented grains (+) nucleated within transition band between two symmetrically oriented S components.